PHYSICAL REVIEW D **90,** 043009 (2014)

Effects of modified gravity on *B*-mode polarization

Luca Amendola, Guillermo Ballesteros, and Valeria Pettorino
Institut für Theoretische Physik, Ruprecht-Karls-Universität Heidelberg, Philosophenweg 16, 69120 Heidelberg, Germany
(Received 20 June 2014; published 20 August 2014)

We explore the impact of modified gravity on *B*-modes, identifying two main separate effects: lensing and propagation of tensor modes. The location of the inflationary peak of the *BB* spectrum depends on the speed of gravitational waves; the amplitude of the lensing contribution depends on the anisotropic stress. We single out these effects using the quasistatic regime and considering models for which the background and the growth of matter perturbations are standard. Using available data we obtain that the gravitational wave speed is compatible with the speed of light and constrained to within about 10%.

DOI: 10.1103/PhysRevD.90.043009 PACS numbers: 95.36.+x, 04.30.-w, 04.50.Kd, 98.80.-k

I. INTRODUCTION

The cosmic microwave background (CMB) is a powerful tool to probe the early universe and the cosmological evolution that followed. Temperature fluctuations have been very well measured by independent experiments [1,2], including the first cosmological data released by the Planck Collaboration [3]. The data are in agreement with the Lambda cold dark matter (ΛCDM) model, although still compatible with scenarios beyond the standard framework (see for example [4]). For this reason, it is important to study the potential of new observables that can help to discriminate different models and constrain them further. An obvious possibility are CMB *B*-modes. Thomson scattering in the presence of primordial fluctuations affects not only the temperature of the CMB but also its polarization. *B*-modes generated by gravitational lensing of the CMB by large-scale structure (LSS) have been observed by two independent teams [5,6]. In addition, the BICEP2 Collaboration has recently claimed the detection of a *B*-mode signal in the CMB (around $\ell \sim 80$), interpreted by the team as the imprint of primordial gravitational waves from inflation [7]. Whether this is indeed the case will depend on the analysis of independent probes, the cross correlation of data at different frequencies and a careful check of foregrounds of polarized dust emission [2,8,9].

Cosmological models in which gravity is modified with respect to Einstein's general relativity (GR) affect the CMB spectra in several ways [10], for example through the late integrated Sachs-Wolfe (ISW) effect [11] and CMB lensing of the temperature spectrum [12,13]. In this paper we study how modified gravity (MG) affects *B*-mode spectra and identify two main observable effects.

The first effect concerns the lensing contribution to *B*-modes and is generated by the anisotropic stress that characterizes modified gravity theories. Gravitational lensing of the CMB by the LSS affects temperature anisotropies and its "electric" (E) and "magnetic" (B) polarized components [14]. The presence of anisotropic stress in MG generically affects the lensing potential and changes the *TT*, *EE* and *BB* spectra (and the cross spectra) with respect to those predicted by GR and ΛCDM.

The second effect is related to the speed c_T of gravitational waves, which can change the peak position of primordial *B*-modes because c_T determines their epoch of horizon crossing. Once foreground emission will be under control, these two effects will give a novel handle for using future *B*-mode measurements as a tool to test MG.

There are important difficulties that arise in trying to test these two effects. First of all, most MG models affect at the same time the lensing potential and the matter Poisson equation, thereby a change in the polarization spectra will typically appear associated to a modification of the growth rate of scalar perturbations. Since the latter begins to be considerably constrained by the current data (see e.g. [15]) and the temperature spectrum of scalar perturbations in the CMB is very well determined [16], it could be naively expected that a substantial modification of the *BB* spectrum would also imply a large imprint in the growth of structures or the *TT* spectrum. In addition, there is a large variety of MG models (see for example [17–19]) and adapting a CMB Boltzmann code for a significant fraction of them is a daunting task. Conversely, restricting the analysis to a narrow subset of cases would reduce the appeal of a study of *B*-modes in MG.

In this paper we propose to bypass these problems by adopting a radical strategy. We will focus on MG models with a single extra scalar degree of freedom in the linear quasistatic (QS) regime, i.e. taking the large k limit and neglecting the time derivatives of the potentials. This reduces considerably the complexity of vast classes of models. Concretely, this can be applied to the entire class of Horndeski Lagrangians [20,21], which comprises most viable modified gravity models based on a scalar field, and bimetric gravity models [22]. Furthermore, we assume that the modification of the Poisson equation is negligible, effectively selecting those models whose effect on the

CMB is essentially due to lensing and the propagation of gravitational waves. We also assume that the background behavior is the one of ΛCDM. In other words, we assume that MG only affects those observables related to gravitational lensing and gravitational waves. This choice allows us to test the effects of the anisotropic stress and the sound speed of gravitational waves with a prescription that can be easily implemented in Boltzmann codes.

MG effects are in general time dependent. We can therefore test their impact at various epochs during the history of the Universe (e.g. at decoupling time or at later times). Lensing effects are mostly generated at a redshift of order unity, while the speed of gravitational waves affects the CMB at decoupling time and, to a minor extent, at or before reionization. In the following we will thus treat separately the following cases: MG effects present at all times, only at decoupling, or only at low redshift.

II. MODIFIED GRAVITY IN THE QUASISTATIC LIMIT

Linear perturbations in MG models are often studied in the QS limit, obtained for wave numbers k that are large compared to the inverse sound horizon, and in which the additional degrees of freedom with respect to GR (e.g. a scalar field or a second spin-2 field) do not propagate significantly but rather can be well described by constraint equations (such as the Poisson equation). The existence of a valid QS approximation is not always guaranteed and should be checked on a case by case basis. For instance, it may happen that the scales at which the limit can be attained are well outside the linear regime, or it may occur that the validity of the limit depends on the specific initial conditions for the perturbations. In addition, the QS limit has to be properly defined in order to avoid spurious scale dependencies [23].

Working with a perturbed flat FLRW metric in Newtonian gauge

$$\mathrm{d}s^2 = -(1+2\Psi)\mathrm{d}t^2 + a^2(1+2\Phi)\mathrm{d}x^i\mathrm{d}x^i, \qquad (1)$$

the effects of MG in the QS limit can be generally encoded in two functions [24] that reduce to $Y = \eta = 1$ in ΛCDM:

$$Y(k,a) \equiv -\frac{2k^2\Psi}{3\mathcal{H}^2\Omega_m\delta_m}, \qquad \eta(k,a) \equiv -\frac{\Phi}{\Psi}, \qquad (2)$$

where $\mathcal{H} = aH$ is the conformal Hubble function, δ_m is the matter density contrast and Ω_m is the background matter energy density relative to the critical one. In Eq. (2) the perturbation variables are meant to denote the standard deviations of the respective quantities; therefore Y, η are deterministic functions. The function Y gives an indication of how the growth of matter perturbations is altered with respect to the standard one in GR for large k. The function η depends on the two Newtonian gravitational potentials and therefore effectively on the anisotropic stress.

It has been shown that Y and η take a particularly simple form in broad classes of MG models in which the equations of motion for the perturbations are of second order (for instance, in the Horndeski Lagrangian or in bimetric gravity) [24–27]:

$$Y = h_1\frac{1+(k/\mathcal{H})^2h_5}{1+(k/\mathcal{H})^2h_3}, \qquad \eta = h_2\frac{1+(k/\mathcal{H})^2h_4}{1+(k/\mathcal{H})^2h_5}. \qquad (3)$$

Here h_{1-5} are functions that depend only on time and can be obtained directly from the Lagrangian of the model (see Appendix). Several types of Hordenski Lagrangians that have been studied in detail (see e.g. references in [23]) provide specific examples for which the expressions (3) can be applied.

As discussed in the Introduction, we will focus our attention on models such that $Y = 1$ but $\eta \neq 1$. With this choice we ensure that scalar perturbations obey the standard Poisson equation for large k: therefore on scales below the sound horizon, the growth of scalar perturbations follows the usual one in ΛCDM. This can occur if $h_1 = 1$ and $h_3 \simeq h_5$ (see the Appendix). To simplify our task further, we will also assume that the three remaining h-functions (h_2, h_4 and h_5) can be treated as constants. This amounts to say that their time variation is slow in one Hubble time and it is a reasonable approximation for studying first order scale dependent effects. With this simplification, a very large class of MG models is mapped into three real constants that encode the possible effects of the anisotropic stress. As crude as they may seem, these approximations are a significant improvement with respect to earlier studies of linear perturbations in MG, in which Y and η were often assumed to be pure constants.

The lensing effect of MG can then be easily described by the deviation of η with respect to unity, which we parametrize as follows:

$$1+\eta = 2a_1\frac{1+a_2(k/k_p)^2}{1+a_3(k/k_p)^2}, \qquad (4)$$

where a_1, a_2, a_3 will be assumed to be constant and we will take $k_p = 0.1h/\mathrm{Mpc}$.[1]

III. TENSOR MODES PROPAGATION SPEED

If the anisotropic stress is nonstandard (i.e. $\eta \neq 1$), it can be shown that the tensor modes propagate in a nonstandard way. As discussed earlier, this will modify the CMB spectra and, in particular, the B-modes. The general form of the propagation equation for the transverse-traceless amplitude

[1]As usual, h here is the reduced Hubble constant $h = H_0/100$, where H_0 is the present rate of expansion expressed in km/s/Mpc.

h in Hordenski Lagrangians can be written (see [23,28] and also [29] for a generalization) as[2]

$$\ddot{h} + (3 + \alpha_M) H \dot{h} + c_T^2 \frac{k^2}{a^2} h = 0, \tag{5}$$

where dots represent derivatives with respect to cosmic time and α_M, c_T are functions of time that depend on the specific model; in the standard case one has $\alpha_M = 0$ and the gravitational waves speed c_T equals the speed of light, $c_T = 1$. Notice that the tensor equation is valid in general, not just in the QS limit. In the notation of [23,24] one has

$$\alpha_M = \dot{w}_1 / w_1 H, \tag{6}$$

$$c_T^2 = w_4 / w_1, \tag{7}$$

where w_1, w_4 are in general time-dependent functions explicitly defined in the Appendix that depend on the MG model. Although in principle they can be both nonzero, in the specific case we are investigating here (see Appendix), one has $\alpha_M = 0$ and

$$c_T^2 = w_1 = \frac{1}{2a_1 - 1}. \tag{8}$$

A decrease of c_T moves the horizon crossing of tensor modes to later times and smaller scales; as a consequence, the BB spectrum tensor mode first peak moves to higher ℓs, as we show later on. The position of the tensor B peak is therefore a measure of the gravitational speed at decoupling time.

The speed of gravitational waves can be constrained also with the gravi-Cherenkov effect (see e.g. [30–32]), which gives an extremely tight lower limit but no upper limit. Other possible ways to constrain the graviton speed are reviewed in [33]. However, all these methods apply only locally (or at most within the distance scale of cosmic rays) and/or at the present time; therefore, they are complementary to the observation of B-modes. For other recent analysis on quantum gravity effects see for example [34].

The theoretical BB spectrum shows another peak at $\ell \approx 5$, still to be detected, due to the effects of tensor modes on the scattering during reionization. Also this peak gets shifted for $c_T \neq 1$ as we show below. Its detection, for instance with the proposed satellite mission LiteBIRD[3] [35], could therefore put constraints on the gravitational wave speed before and during reionization.

IV. WEAK LENSING AND CMB SPECTRA

In order to compute the weak lensing of the CMB by LSS in a flat universe, we define the lensing potential ψ from the Weyl potential $\tilde{\Psi} \equiv (\Psi - \Phi)/2$ as follows [14] [note that we are using a different signature for the metric in Eq. (1)]:

$$\psi(\hat{\mathbf{n}}) = 2 \int_0^{\chi_*} d\chi \tilde{\Psi}(\chi \hat{\mathbf{n}}, \tau_0 - \chi) \frac{\chi_* - \chi}{\chi_* \chi}. \tag{9}$$

In this expression, $\hat{\mathbf{n}}$ is a unit vector in three-space that gives the (non-deflected) direction of propagation of a CMB photon, $\tau_0 - \chi$ is the conformal time at which the photon was at position $\chi \hat{\mathbf{n}}$ and χ_* is the conformal distance to the last scattering surface (assuming it is instantaneous).

The deflection angle with respect to the trajectory that the photon would have in a perfectly homogeneous universe is given by the angular derivative of the lensing potential $\alpha = \nabla_{\hat{\mathbf{n}}} \psi(\hat{\mathbf{n}})$. The lensed CMB temperature Θ_L measured in the direction $\hat{\mathbf{n}}$ corresponds to the unlensed temperature Θ in the direction $\hat{\mathbf{n}} + \nabla_{\hat{\mathbf{n}}} \psi$, i.e.

$$\Theta_L(\hat{\mathbf{n}}) = \Theta(\hat{\mathbf{n}} + \nabla_{\hat{\mathbf{n}}} \psi). \tag{10}$$

With the definitions (2) we can write

$$\tilde{\Psi} = \frac{1}{2}(1 + \eta)\Psi \tag{11}$$

and use this relation to express the lensing potential (9) in terms of Ψ and η. We can then write $P_{\tilde{\Psi}} = (1 + \eta)^2 P_\Psi / 4$ where the power spectrum (and similarly the transfer function) of $\tilde{\Psi}$ is written in terms of the one of Ψ, which is related to the matter one by the Poisson equation (2). As noticed before, since the main contribution to CMB lensing comes from a short range in z, peaked around $z \sim 1$ [12,13,36,37], the assumption of constant values for $a_{1,2,3}$ is justified. We can then modify a Boltzmann code to include the effect of MG in the computation of the lensing potential with these approximations.

The power spectrum C_l^ψ of the lensing potential at a given $\hat{\mathbf{n}}$ is

$$\langle \psi_{lm} \psi_{l'm'} \rangle = \delta_{ll'} \delta_{mm'} C_l^\psi, \tag{12}$$

where ψ_{lm} are the coefficients of the expansion of ψ in spherical harmonics: $\psi = \sum_{lm} \psi_{lm} Y_{lm}$. This power spectrum can be expressed as [14]:

$$C_\ell^\psi = 16\pi \int \frac{dk}{k} \mathcal{P}_\mathcal{R}(k) \left[\int_0^{\chi_*} d\chi T_{\tilde{\Psi}}(k; \tau_0 - \chi) j_l(k\chi) \frac{\chi_* - \chi}{\chi_* \chi} \right]^2, \tag{13}$$

where $\mathcal{P}_{\tilde{\Psi}} = \mathcal{P}_\mathcal{R} T_{\tilde{\Psi}}$ and $j_\ell(r) = \sqrt{\pi/2r} J_{l+1/2}(r)$, being $J_l(r)$ is the lth Bessel function of the first kind. The transfer function $T_{\tilde{\Psi}}(k; \tau_0 - \chi)$ propagates the lensing potential (9) forward in time. $\mathcal{P}_\mathcal{R}(k)$ denotes the power spectrum of the primordial curvature perturbation $\mathcal{R}$ at the last scattering surface. Following Eq. (11), we can then account for the effect of MG by introducing a $(1 + \eta)/2$ factor inside

[2]We thank M. Kunz, I. Saltas, and I. Sawicki for discussing with us the structure of this equation.

[3]http://litebird.jp/.

the χ integral of (13). Again, for $\eta = 1$, the integral is the standard one.

Before doing the full calculation with a Boltzmann code, we can get some insight of the MG effect in the region of relevance for the expected primordial B-mode peak for large scales ($\ell \ll 1000$) [14]. In this limit and at lowest order in C_ℓ^ψ, the lensed B-mode spectrum $\tilde{C}_l^B$ is approximately independent of ℓ [14]:

$$\tilde{C}_\ell^B \simeq \frac{1}{4}\int d\ell' \ell'^5 C_{\ell'}^\psi C_{\ell'}^E, \tag{14}$$

where C_ℓ^E is the unlensed E-mode spectrum. Since C_ℓ^ψ enters linearly in (14), we see that in modified gravity the lensing contribution to the B-mode spectrum gets enhanced at large scales by $(1+\eta)^2/4$, with respect to ΛCDM.

Since we are deriving the lensing MG effects in the QS limit, i.e. at subhorizon scales, it is necessary to check the consistency of our assumption. A comoving mode k translates through the Limber approximation into a multipole

$$\ell \approx \pi r(z) k. \tag{15}$$

One finds that for a standard ΛCDM background, $k/\mathcal{H} > 10$ up to $z = 7$, and $k/\mathcal{H} > 5$ up to $z = 20$, assuming $\ell \geq 100$, which is where most of the BB lensing signal is expected. Since the lensing effect comes from z of a few at most [14], we expect the quasistatic approximation to be acceptable.

As we already mentioned, we are neglecting the impact of MG on the ISW effect. Although $Y = 1$ means that there is no effect on the matter perturbation growth, there will be a change in the ISW due to the fact that photons see both potentials Ψ, Φ, just as in the lensing case. However, contrary to lensing, the ISW has a non-negligible impact on the temperature CMB fluctuations at superhorizon scales, where our quasistatic approximation is not reliable. We can obtain a rough estimate of the MG effect on the low-ℓ TT spectrum by considering that the ISW contribution is negligible at $\ell > 30$. Then we find that it amounts to less than 20% (see e.g. [38]) at $\ell > 10$, and rises up to 50% for $\ell = 2$. The MG effects are again proportional to $(1+\eta)^2$, although at these scales the form of η is no longer given by the QS expression. Nevertheless, assuming $a_1 \approx 1.3$ (see our best fit case below), we see that the ISW should be increased by 69%, which means the total TT spectrum should increase by 14% at $\ell \approx 10$, and up to 35% at the quadrupole. This is a non-negligible effect but it is well within the cosmic variance. Moreover, it might be possible to absorb it by slight adjustments of other cosmological parameters, although we are not going to explore this possibility in depth in this paper.

Let us just briefly point out what would be the effect of the MG model we consider on the determination of neutrino masses and the total number of relativistic species. As it is well known (see e.g. [39]), the effect of small neutrino masses on the CMB power spectrum takes place via secondary anisotropies and is multipole dependent. In standard ΛCDM, a total neutrino mass of the order of $\sum m_\nu \simeq 0.5$ eV reduces the CMB C_l with respect to the case $\sum m_\nu = 0$ by at most ∼8% for $10 < \ell < 20$, due to the late time ISW. For larger values of ℓ, the early time ISW decreases the C_l by smaller amount (around 2% up to $\ell \sim 100$) and then increases it by approximately 1% (for $100 < \ell < 500$). As we have just explained the $(1+\eta)^2$ factor introduced in the ISW by the modification of gravity we consider in this work tends to enhance the C_l with respect to ΛCDM for all ℓ. Therefore, for small multipoles ($\ell < 100$) it would go on the opposite direction as that of $\sum m_\nu$, whereas it would enhance the effect of massive neutrinos for $100 < \ell < 500$ (where the early time ISW introduced by $\sum m_\nu$ is rather small). If a $(1+\eta)^2$ factor was present in the CMB, the net overall effect would be an increased ISW that could be approximately compensated by a higher value of $\sum m_\nu$.

On the other hand, the main CMB effect of a larger number of effective relativistic species $N_{\rm eff}$ with respect to its standard value of 3.046 is due to a delayed time of matter-radiation equality, which results in a vertical shift of the CMB peaks with respect to the first one [40]. Concretely, it introduces a shift of the order of $\Delta C_l/C_l \simeq -0.072\Delta N_{\rm eff}$. This means that a $(1+\eta)^2$ ISW change can have a similar effect as that of a reduced number of relativistic species. In conclusion, the kind of MG that we consider can affect the determination of both the total neutrino mass and the number of relativistic species. A detailed study of the degeneracies of these effects could be the object of future work.

In any case, in order not to bias our results, we decided to bypass this problem in the data analysis below by cutting all the multipoles $\ell < 100$ in the TT and TE spectra. This slightly enlarges our errors but avoids using the incorrectly modeled low-ℓ tail of the temperature spectrum. We conclude this paragraph by noting that also weak lensing of the matter power spectrum can be used to test modified gravity models [41] and should be seen as a complementary probe with respect to the lensing on B-mode polarization. On the other hand, we have checked that the corresponding TT and EE spectra are very little affected by the kind of modification of gravity that we study, so that the main contribution of MG is on B-modes.

V. RESULTS

In order to test how modified gravity affects the CMB spectra, we have modified the publicly available Boltzmann code CAMB.[4] Given the assumptions described in Sec. II,

[4] http://camb.info/.

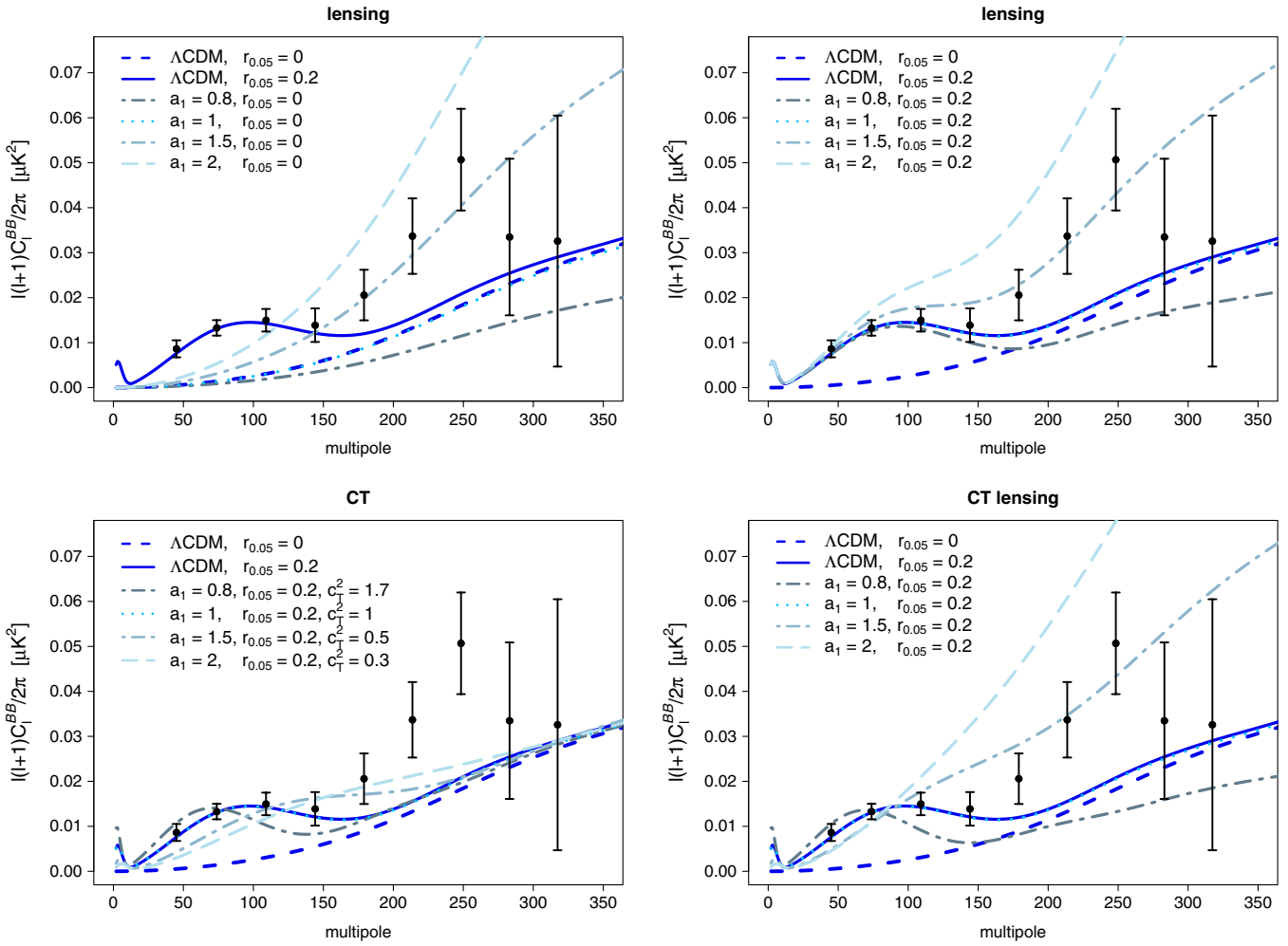

FIG. 1 (color online). BB power spectrum for MG models. In the top panels we show the effect of a lensing correction for $r = 0$ and $r = 0.2$ respectively. In the bottom left panel we plot the case in which the "CT"' correction on the speed of gravitational waves is active (while the lensing is standard). In the bottom right panel we activate both effects. In all cases for simplicity we assume $a_2 = a_3$ and different values of the a_1 parameter. The corresponding values of c_T^2 are written in the bottom left panel and are related to a_1 via Eq. (8). For comparison, the predictions for ΛCDM with $r = 0$ (short dashed, blue) and $r = 0.2$ (solid, blue) are also shown. The black dots are the data points from BICEP2.

we do not need to modify the background, which is assumed to be ΛCDM. Within CAMB, we apply two sets of corrections to perturbations, which can be activated separately or simultaneously:

(i) we modify the lensing potential as described in Eq. (11), which then depends on the a_1, a_2, a_3 parameters;
(ii) we modify the tensor propagation equation as described in Eq. (5). This modification only depends on a_1.

We have included the three new parameters in COSMOMC [42]. Both CAMB and COSMOMC used for this paper are the ones from the March 2014 version. After checking that for $a_1 = 1$ and $a_2 = a_3$ we recover standard ΛCDM, we have then tested separately three cases: when MG effects are present at all times and therefore both on lensing and on the gravitational wave speed (we refer to this case as "CT + lensing"), when they are present only at decoupling and therefore only on the tensor speed (CT), or only at low redshift ("lensing").

To illustrate the effects of MG on the BB polarization we show its spectrum in Figs. 1–3 for various choices of a_1 while we always fix $a_2 = a_3$, just for illustration.

In Fig. 1 we plot the BB spectrum for the three effects (lensing, CT, CT + lensing). The top panels refer to the lensing case for a tensor-to-scalar ratio $r_{0.05} = 0$ and $r_{0.05} = 0.2$ respectively. The ΛCDM is also shown for reference for both values of $r_{0.05}$. As expected, increasing the value of a_1 effectively increases η and therefore the integrand in Eq. (13): the lensing contribution therefore

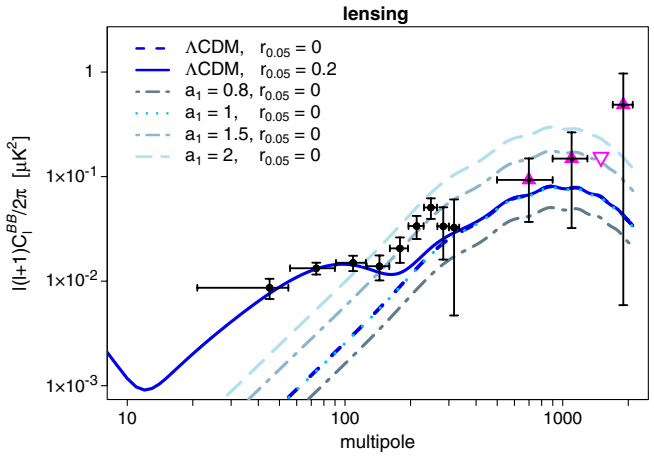

FIG. 2 (color online). The theoretical predictions of Fig. 1, first panel, are shown here for a larger ℓ range with a log scale. The horizontal error bars associated to the BICEP2 data points correspond to the interval $(\ell_{\rm min}, \ell_{\rm max})$ from the data currently available from the BICEP2 Collaboration. For reference, although not used in this analysis, we also overplot data from POLARBEAR (magenta, triangular points). The third of these points is given as an upper limit at 2 standard deviations.

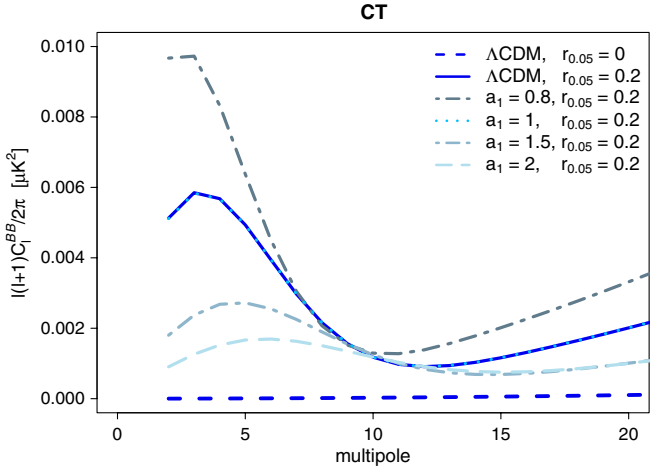

FIG. 3 (color online). Zoom at low multipoles of the BB spectrum of Fig. 1, bottom left panel. A CT effect, i.e. a change in the speed of gravitational waves, is expected to modify the reionization peak in B-modes.

increases in amplitude and extends to smaller multipoles than expected for the corresponding ΛCDM. The position of the primordial peak is however not affected (although its amplitude also receives a contribution from MG). The bottom left panel shows the BB spectra when only the CT effect is active: in this case, the speed of gravitational waves changes with the inverse of a_1 as described in Eq. (8): a value of a_1 smaller (larger) than one increases (decreases) the speed of gravitational waves with respect to ΛCDM and shifts the expected position of the primordial peak to smaller (larger) multipoles. When both effects are active, as in the bottom right panel, both the lensing amplitude and the shift in peak position can occur. In all panels we also overplot for reference the recently released data points of BICEP2.[5] We note that the corresponding TT and EE spectra are very little affected by these changes, so that in our model the main contribution of MG is on B-modes. In Fig. 5 we replot the lensing case, as in Fig. 1 top left panel, for $r_{0.05} = 0$ and a wider range in scales, up to $\ell = 2000$, to show how the lensing predictions for MG compare with the available data from POLARBEAR,[6] although we do not use them in our analysis. Notice that if we took BICEP2 data at face value, while the "bump" around $\ell \sim 80$ is best rendered by a nonzero tensor-to-scalar ratio ($r = 0.2$) in ΛCDM, the location of the upper points is qualitatively in good agreement with a modification of gravity represented by $a_1 \approx 1.5$.

[5]http://bicepkeck.org/B2_3yr_bandpowers_20140314.txt.

[6]http://lambda.gsfc.nasa.gov/product/suborbit/polarbear_prod_table.cfm.

Finally, in Fig. 3, we zoom in the low-ℓ region in order to emphasize the effect of a change in c_T on the reionization peak. Interestingly, future measurements of the reionization peak by experiments like those in Refs. [43–47] could be used to discriminate MG theories. For example, the satellite mission LiteBIRD [35] would have a sensitivity to characterize the tensor-to-scalar ratio r with an uncertainty of $\delta r \sim 0.001$. At these scales the lensing contribution is negligible and the only modification comes from the correction in the speed of gravitational waves.

We then proceed with Monte Carlo simulations using available data to test the parameters of our implementation of MG. We use WMAP9 data [48], ACT [49] +SPT [50] and the data from BICEP2 [7] on B-modes polarization. We enforce the inflationary consistency relation $n_t \simeq -r/8$ for the tensor spectral index n_t. We perform different runs, including the three cases illustrated before: lensing modification, CT, CT + lensing modifications. Results are illustrated in Table I. As the values for a_2 and a_3 can in principle span several orders of magnitude, we use for convenience the logarithm of these quantities. The parameters a_2 and a_3 play no role in CT and are essentially unconstrained also including the lensing MG effect. Provided that the foreground contributions are under control, B-modes polarization will be however a very good probe to test the a_1 parameter, i.e. the anisotropic stress and the speed of gravitational waves.

In Fig. 4 we show 1D posterior contours for a selection of cosmological parameters and different runs. Here it becomes clearer that a_1 is mainly constrained by the lensing contribution, while CT gives much larger uncertainty. This can be seen intuitively from Fig. 1: CT influences both the amplitude and the position of the

TABLE I. Mean values ± standard deviation for a selection of parameters. Both columns refer to the combination of data sets WMAP + HighL + BICEP2. For $\log(a_2)$ and $\log(a_3)$ parameters we write the 95% upper limit; these parameters are essentially not constrained.

Data sets: WMAP9 + HighL + BICEP2				
Parameter	ΛCDM	MG (lensing)	MG (CT)	MG (CT + lensing)
a_1	⋯	1.30 ± 0.16	2.89 ± 1.21	1.28 ± 0.15
$\log_{10} a_2$	⋯	<0.30	⋯	< -1.12
$\log_{10} a_3$	⋯	<0.37	⋯	< -0.11
$r_{0.05}$	0.21 ± 0.05	0.19 ± 0.05	0.35 ± 0.11	0.21 ± 0.05
$r_{0.002}$	0.23 ± 0.06	0.21 ± 0.06	0.43 ± 0.17	0.23 ± 0.07
H_0	72.0 ± 2.2	73.7 ± 2.4	73.0 ± 2.4	73.9 ± 2.4
n_s	0.998 ± 0.013	1.000 ± 0.014	1.012 ± 0.016	1.006 ± 0.015
$-\log \mathcal{L}$	4146	4142	4145	4143

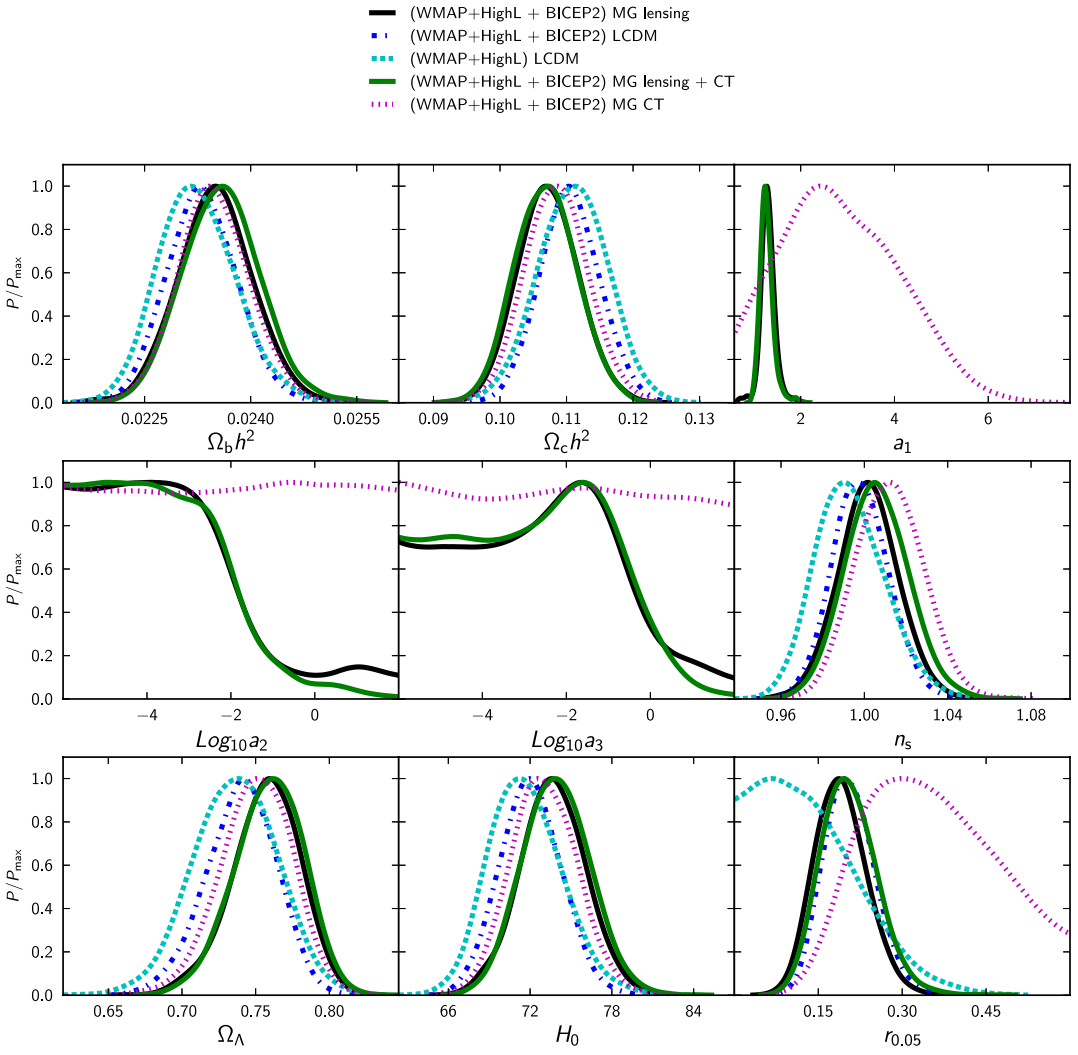

FIG. 4 (color online). One-dimensional posterior contours for a selection of cosmological parameters. We compare the three cases in which: lensing is modified (solid, black line), CT is modified (dotted magenta line), CT and lensing are both modified (light solid, green line). We overplot also the case of ΛCDM for comparison (dot dashed, blue line).

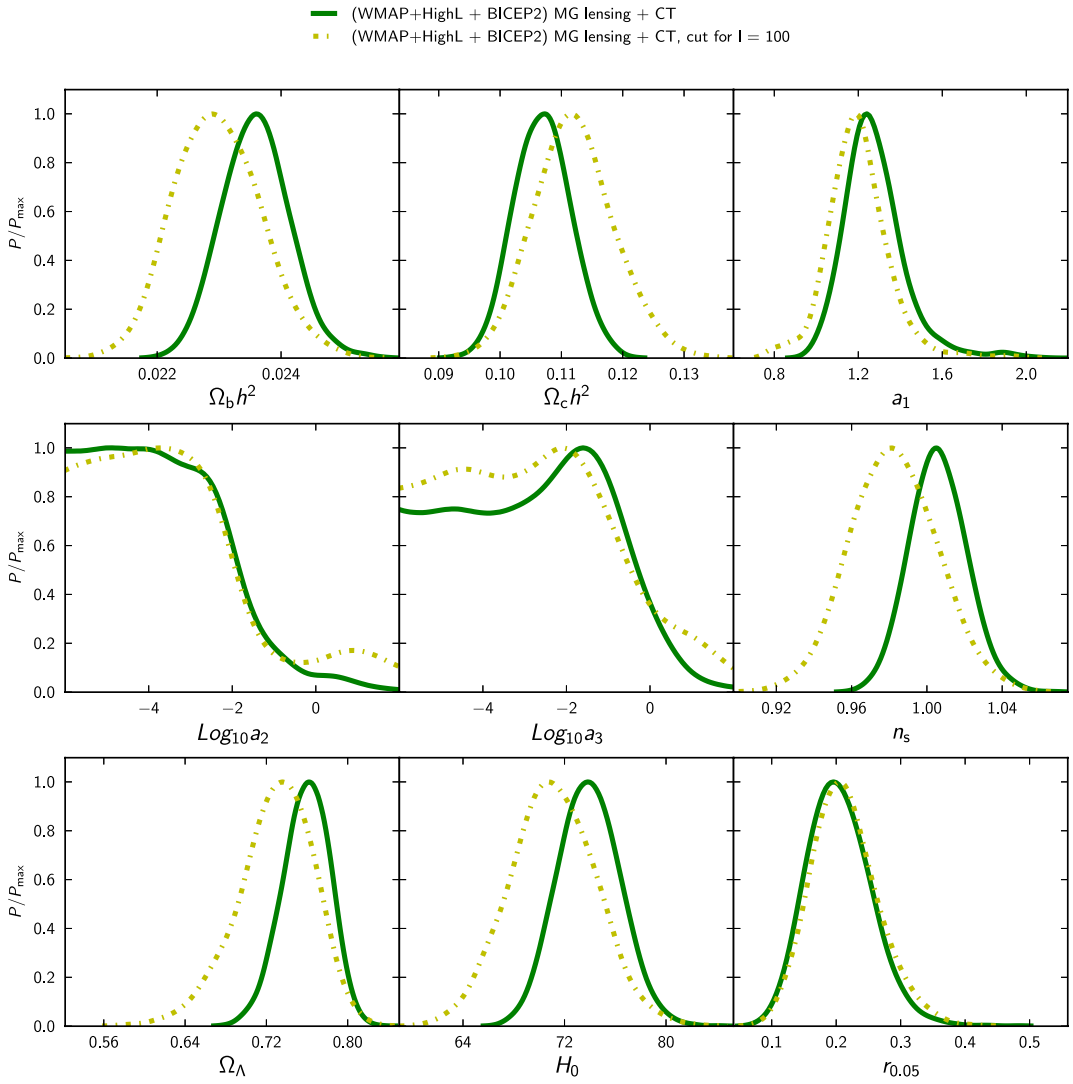

FIG. 5 (color online). One-dimensional posterior contours for a selection of cosmological parameters. For the case in which both CT and lensing are both modified, we compare the constraints obtained using all multipoles (solid, green line), to the case in which we cut all multipoles $\ell < 100$ in TT and TE (dash-dotted, light green).

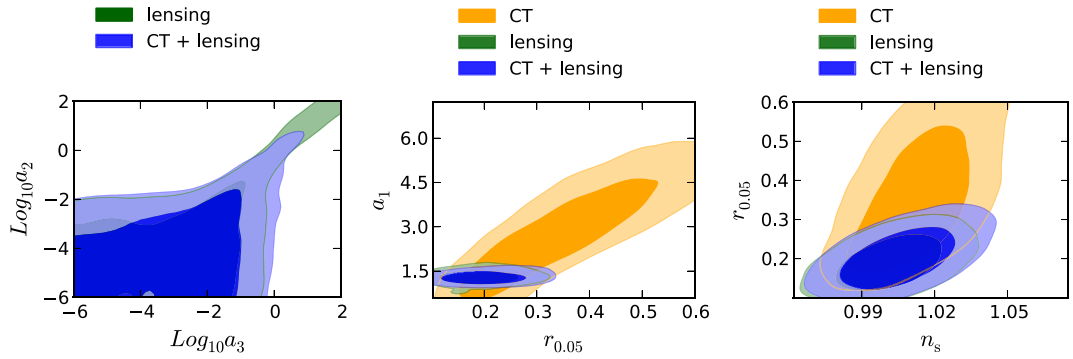

FIG. 6 (color online). 2D posterior contours for a selection of cosmological parameters and the three cases in which lensing only is modified (green contours), CT only is modified (orange/light contours), CT and lensing are both modified (blue/darker contours). The case including CT only does not depend on a_2 and a_3 parameters. As before, we consider the data combination WMAP + HighL + BICEP2.

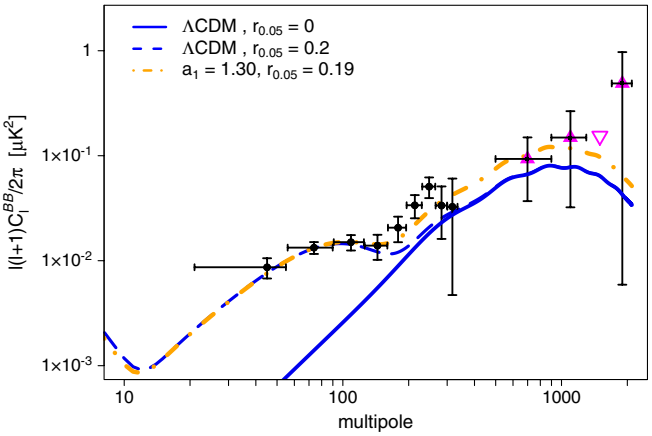

FIG. 7 (color online). Best fits from Table 1. MG with $r \neq 0$ is shown (dash-dotted, orange) together with ΛCDM assuming also $r \neq 0$ (dashed, blue). For comparison we also show ΛCDM with $r = 0$ (blue). As in Fig. 2, we show the data points of POLARBEAR (magenta triangles) in addition to those of BICEP2. The error in the abscissa associated to the BICEP2 data points corresponds to the interval $(\ell_{\rm min}, \ell_{\rm max})$ from the release by the BICEP2 team. The third point from POLARBEAR is plotted as an upper limit at 2 standard deviations. We recall that POLARBEAR data are not used in the analysis and are only shown here for reference.

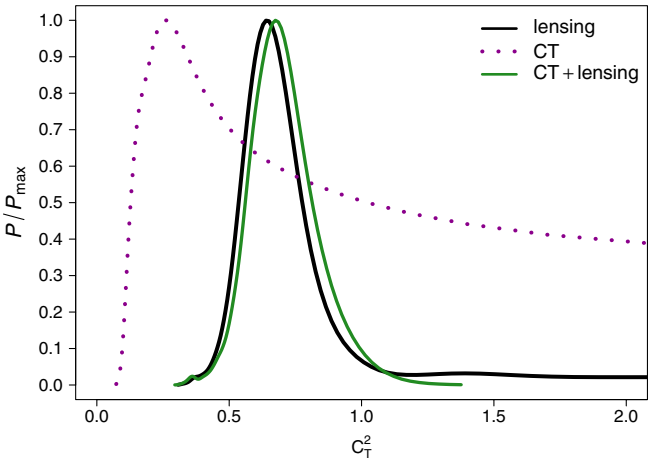

FIG. 8 (color online). Speed of gravitational waves, as obtained remapping the constraints on a_1 for the three different effects considered in this paper: lensing (dark solid, black line), CT (dotted magenta), CT + lensing (lighter solid, green). $c_T^2 = 1$ corresponds to the standard value.

BB spectrum and is able to fit the data for a larger range in a_1.

In order to check the validity of the QS limit, we test the effect of the incorrectly modeled low-ℓ part of the TT spectrum by redoing the MCMC simulation cutting the first 100 multipoles in the TT and TE spectra. A comparison of the run with and without cut is shown in Fig. 5. As we see, while parameters like n_s and H_0 are affected by the cut, constraints on a_1 do not depend on the cut; i.e. they do not depend much on the low-ℓ multipoles in the temperature spectra. This is reassuring as it shows that the QS limit and its simplest numerical implementation may be sufficient to test MG theories.

In Fig. 6 we show the comparison of the 2D posterior contours for the three effects. In addition to the considerations already done above, we notice here that a_2 and a_3 are degenerate and tend to align along the direction $a_2 = a_3$. This particular direction removes any scale dependence in the expression for η in (4).

In Fig. 7 we redo Fig. 3 for $a_1 = 1.30$, corresponding to the mean (and best fit) of modified gravity, for the lensing case shown in the plot.

Finally, we remap the constraints obtained for the various runs on a_1 into c_T, the speed of gravitational waves. The resulting 1D contours are shown in Fig. 8. We find that $c_T = 0.8 \pm 0.07$ from CT + lensing. Using CT alone the constraint is much weaker: $c_T \gtrsim 0.4$ at 2σ. The reason for this behavior can be understood by looking at Fig. 6. In the central panel one can see that a_1 (or equivalently c_T) is quite degenerate with $r_{0.05}$ if lensing is not taken into account. This is because a shift of the tensor peak towards higher ℓs can be partially compensated by an increase of $r_{0.05}$. In other words, a_1 (or c_T) could be determined by the tensor peak position (see the bottom-left panel of Fig. 1) which is not firmly established by the current data. However, c_T changes the lensing amplitude in a significant way (see Fig. 1, top-right panel) and is therefore well measured by lensing alone.

VI. CONCLUSIONS

The polarized light from the last scattering surface carries important information in addition to the temperature anisotropy. Not only it helps constraining the cosmological parameters but it also allows us to separate the effects of primordial gravitational waves from scalar perturbations, both predicted by inflationary models. Current experiments [6,7,51] are already providing results which will soon be cross tested by Planck. Future observations [43–47] will keep improving our knowledge of CMB polarization. B-modes, once foregrounds are accounted for, are particularly important in this context since they contain both the imprint of primordial gravitational waves and the one from gravitational lensing induced by large-scale structure. In a sense, B-modes are the ultimate test of gravity at cosmological scales since they probe two genuinely general relativistic effects.

Modifications of gravity have been mainly proposed to describe the late time acceleration of the universe (see e.g. [52] for a review) but they have also been studied as a possibility for driving primordial inflation (e.g. [53–56]). In any case, it is conceivable that some extra degrees of freedom affect gravity at early times, see for instance [57].

In this paper we investigated how B-modes can be employed to test gravity at early times and at cosmological scales. Both lensing and gravitational wave propagation depend on the features of gravity and one can use them to constrain its properties. It is remarkable that both effects depend on the amount of anisotropic stress η, which in general differs from the standard value of unity in modified gravity. To simplify our study, we single out the effects that depend on η alone by selecting models in which the background and the matter perturbation growth are exactly standard. Moreover, we work in the quasistatic limit, in which all the modified gravity effects can be embodied in just two arbitrary functions of time and space. In a vast class of models (the Horndeski Lagrangian [20] and in bimetric gravity [22]), these two functions take a particularly simple form, given by Eq. (3).

We show by a Monte Carlo analysis with real data that it is indeed possible to constrain the anisotropic stress and the gravitational wave speed with B-modes. Although the particular values we obtain here are to be taken with great caution because the B-mode available data are still under close scrutiny, future data has great potential for providing tight constraints on MG.

Several of the assumptions we adopted for simplicity in this work can be lifted relatively easily: one can for instance remove the assumption of constant MG parameters and work with the full equations rather than with their quasistatic limit. This will be addressed in future works.

ACKNOWLEDGMENTS

We acknowledge support from the TRR33—The Dark Universe—DFG Grant. We thank Emilio Bellini, Diego Blas, Alicia Bueno-Belloso, Martin Kunz, Ippocratis Saltas, Ignacy Sawicki, and Licia Verde for fruitful discussions. We also thank Francesco Montanari for useful comments on a draft version of this work.

Note added.—Shortly after our work was made public, a related study on the speed of gravitational waves also appeared, see [58].

APPENDIX: ANISOTROPIC STRESS WITHOUT MODIFIED GROWTH

One may wonder whether taking $\eta \neq 1$ and $Y = 1$ at the same time is consistent since it can be expected that a general modification of gravity would induce a change in both Poisson's equation and the relation between the metric potentials, Ψ and Φ. Although this is indeed the general case, it is possible to find situations in the QS limit that produce an anisotropic stress component, but do not modify Newton's constant. We will illustrate this with an example.

The action

$$S = \int \mathrm{d}^4x\sqrt{-g}\left(\frac{1}{2}R + \mathcal{L}_x + \mathcal{L}_\mathrm{m}\right) \tag{A1}$$

describes the behavior of matter (with Lagrangian density $\mathcal{L}_\mathrm{m}$) in a modification of GR given by $\mathcal{L}_\mathrm{x}$. In the case of Hordenski MG theories, the modification of GR is given by a scalar field ϕ with $\mathcal{L}_\mathrm{x} = \sum_{i=2}^{5}\mathcal{L}_i$, where

$$\mathcal{L}_2 = K(\phi, X), \tag{A2}$$

$$\mathcal{L}_3 = -G_3(\phi, X)\Box\phi, \tag{A3}$$

$$\mathcal{L}_4 = G_4(\phi, X)R + G_{4,X}[(\Box\phi)^2 - (\nabla_\mu\nabla_\nu\phi)(\nabla^\mu\nabla^\nu\phi)], \tag{A4}$$

$$\begin{aligned}\mathcal{L}_5 = {} & G_5(\phi, X)G_{\mu\nu}\nabla^\mu\nabla^\nu\phi \\ & - \frac{G_{5,X}}{6}[(\Box\phi)^3 - 3(\Box\phi)(\nabla_\mu\nabla_\nu\phi)(\nabla^\mu\nabla^\nu\phi) \\ & + 2(\nabla^\mu\nabla_\alpha\phi)(\nabla^\alpha\nabla_\beta\phi)(\nabla^\beta\nabla_\mu\phi)].\end{aligned} \tag{A5}$$

The functions K and G_i are in principle arbitrary and $X = -\partial_\mu\phi\partial^\mu\phi/2$ is the standard kinetic term.

The QS limit of the equations of motion derived from this action are characterized by the functions h_i appearing in Eq. (3). They can be expressed as

$$\begin{aligned}
h_1 &\equiv \frac{w_4}{w_1^2} = \frac{c_\mathrm{T}^2}{w_1}, \qquad h_2 \equiv \frac{w_1}{w_4} = c_\mathrm{T}^{-2}, \\
h_3 &\equiv \frac{H^2}{2XM^2}\frac{2w_1^2w_2H - w_2^2w_4 + 4w_1w_2\dot{w}_1 - 2w_1^2(\dot{w}_2 + \rho_\mathrm{m})}{2w_1^2}, \\
h_4 &\equiv \frac{H^2}{2XM^2}\frac{2w_1^2H^2 - w_2w_4H + 2w_1\dot{w}_1H + w_2\dot{w}_1 - w_1(\dot{w}_2 + \rho_\mathrm{m})}{w_1}, \\
h_5 &\equiv \frac{H^2}{2XM^2}\frac{2w_1^2H^2 - w_2w_4H + 4w_1\dot{w}_1H + 2\dot{w_1}^2 - w_4(\dot{w}_2 + \rho_\mathrm{m})}{w_4},
\end{aligned} \tag{A6}$$

being

$$
\begin{aligned}
w_1 &\equiv 1 + 2(G_4 - 2XG_{4,X} + XG_{5,\phi} - \dot{\phi}XHG_{5,X}),\\
w_2 &\equiv -2\dot{\phi}(XG_{3,X} - G_{4,\phi} - 2XG_{4,\phi X}) + 2H(w_1 - 4X(G_{4,X} + 2XG_{4,XX} - G_{5,\phi} - XG_{5,\phi X})) - 2\dot{\phi}XH^2(3G_{5,X} + 2XG_{5,XX}),\\
w_3 &\equiv 3X(K_{,X} + 2XK_{,XX} - 2G_{3,\phi} - 2XG_{3,\phi X}) + 18\dot{\phi}XH(2G_{3,X} + XG_{3,XX}) - 18\dot{\phi}H(G_{4,\phi} + 5XG_{4,\phi X} + 2X^2G_{4,\phi XX})\\
&\quad - 18H^2(1 + G_4 - 7XG_{4,X} - 16X^2G_{4,XX} - 4X^3G_{4,XXX}) - 18XH^2(6G_{5,\phi} + 9XG_{5,\phi X} + 2X^2G_{5,\phi XX})\\
&\quad + 6\dot{\phi}XH^3(15G_{5,X} + 13XG_{5,XX} + 2X^2G_{5,XXX}),\\
w_4 &\equiv 1 + 2(G_4 - XG_{5,\phi} - XG_{5,X}\ddot{\phi}),
\end{aligned}
\tag{A7}
$$

and

$$
M^2\dot{\phi} = 3H(P_{x,\phi} + \rho_{x,\phi}) + \dot{\rho}_{x,\phi} \tag{A8}
$$

$$
\begin{aligned}
\rho_x &= 3H^2(1 - w_1) + 2XK_{,X} - K - 2XG_{3,\phi} + 6\dot{\phi}H(XG_{3,X} - G_{4,\phi} - 2XG_{4,\phi X})\\
&\quad + 12H^2X(G_{4,X} + 2XG_{4,XX} - G_{5,\phi} - XG_{5,\phi X}) + 4\dot{\phi}XH^3(G_{5,X} + XG_{5,XX}),\\
P_x &= -(3H^2 + 2\dot{H})(1 - w_1) + K - 2XG_{3,\phi} + 4XG_{4,\phi\phi} + 2\dot{\phi}Hw_{1,\phi} - 4X^2H^2G_{5,\phi X}\\
&\quad + 2\dot{\phi}XH^3G_{5,X} + \ddot{\phi}(w_2 - 2Hw_1)/\dot{\phi}.
\end{aligned}
\tag{A9}
$$

We see from Eq. (2) that in order to get $\eta \neq 1$ and $Y = 1$ in the QS limit we must impose

$$
h_3 = h_5 \tag{A10}
$$

$$
h_1 = 1. \tag{A11}
$$

The condition (A11) enforces

$$
w_4 = w_1^2. \tag{A12}
$$

Then, the condition (A10) becomes a relation between the Hubble parameter H and the functions w_1 and w_2:

$$
\dot{w}_1 = w_1\left(\frac{w_2}{2} - H\right). \tag{A13}
$$

If we impose

$$
G_{3,X} = 0 \qquad G_{4,\phi} = 0 \qquad G_{5,X} = 0, \tag{A14}
$$

the equations $w_2 = 2H$ and $w_4 = w_1^2$ are equivalent to

$$
G_4 + X(3G_{5,\phi} - 4G_{4,X} - 4XG_{4,XX}) = 0 \tag{A15}
$$

$$
\begin{aligned}
&2(G_4 - XG_{4,X})^2 + X^2(9 + 8G_4 - 8XG_{4,X})G_{4,XX}\\
&\quad + 8X^4G_{4,XX}^2 = 0.
\end{aligned}
\tag{A16}
$$

Under these conditions, the function w_1 takes the form

$$
w_1 = 1 + \frac{4}{3}(G_4 - XG_{4,X} + 2X^2G_{4,XX}). \tag{A17}
$$

Then, if $G_5 \propto \phi$ and the field evolves keeping X constant, Eqs. (A15) and (A16) become algebraic constraints and w_1 can be different from 1 (as required to have a nontrivial η). With this choice, $Y = 1$ and $\eta = 1/w_1$ and constant.

Assuming that the matter component has zero pressure and ρ_m energy density, the equations of motion in the background (the Friedmann equations) are in this case

$$
\rho_m - K + 2XK_{,X} - 2XG_{3,\phi} = 3H^2 \tag{A18}
$$

$$
\eta(-K + 2XG_{3,\phi}) = 3H^2 + 2\dot{H}. \tag{A19}
$$

Notice that if only matter is present, we recover the standard equations $\rho_m = 3H^2$ and $3H^2 + 2\dot{H} = 0$.

Equations (A18) and (A19) can be combined into

$$
\frac{dH^2}{d\ln a} + 3(1 + \eta)H^2 = \eta(\rho_m - 2K + 2XK_{,X}), \tag{A20}
$$

which allows us to get H for a given ρ_m and $K(\phi, X)$. In particular, a ΛCDM evolution for the background can be obtained provided that the matter density today is

$$
\Omega_m^0 = 1 - \frac{2\eta(XK_{,X} - K)}{3(1 + \eta)}, \tag{A21}
$$

and that

$$
2(1 + \eta)XG_{3,\phi} = 2K_{,X}X + K(\eta - 1). \tag{A22}
$$

Since η is constant, these conditions can be achieved if G_3 is linear in ϕ, K depends only on X and the field evolves keeping X constant. We have to check also the

Klein-Gordon equation for ϕ (see [28]), which under these conditions takes the following form:

$$\frac{d}{d\ln a}(a^3 J) = 0, \tag{A23}$$

where

$$J = \sqrt{2X}(K_{,X} - 2G_{3,\phi} + 6H^2(G_{4,X} + 2XG_{4,XX} - G_{5,\phi})). \tag{A24}$$

We obtain that (A23) is satisfied if $J \propto a^{-3}$ which, for a ΛCDM background, implies

$$K_{,X} - 2G_{3,\phi} = 6(\Omega_{m0} - 1)(G_{4,X} + 2XG_{4,XX} - G_{5,\phi}). \tag{A25}$$

Therefore, we see that the background evolution is exactly ΛCDM, the effective Newton constant has the standard value (i.e. $Y = 1$) but the anisotropic stress can be different from unity.

Let us finally give a specific case for which these conditions are satisfied. If, for instance, we take

$$K = \beta e^{mX}, \qquad G_3 = 0, \qquad G_4 = \alpha\frac{1+X^n}{1+X}, \qquad G_5 = 0, \tag{A26}$$

where X is in units of H_0^2 and α, β, n and m are constants, Eqs. (A15), (A16), (A21), (A22) and (A25) can be simultaneously solved, provided X is suitably chosen. For instance, if we choose $\alpha = -0.286, X = 1.082, n = 1.360$ and put $\Omega_m^0 = 1/3$ we obtain $\beta = -1.70, m = -0.251$ and $c_T \approx 0.8$ as in our best fit, with the anisotropic stress different from unity and equal to $\eta \approx 1.55$. Although this is just a minimal toy model without any special physical significance, it nevertheless shows that a MG model with the properties we have employed in this paper is indeed possible. More general cases in which, for instance, G_3, G_5 are not zero and η is time and scale dependent also exist. Many other examples in which $Y = 1 + \mathcal{O}(10^{-N})$, where N is large, can be constructed as well.

[1] P. A. R. Ade, N. Aghanim, C. Armitage-Caplan, M. Arnaud, M. Ashdown, F. Atrio-Barandela, J. Aumont, C. Baccigalupi, A. J. Banday *et al.* (Planck Collaboration), arXiv:1303.5076.
[2] C. L. Bennett, D. Larson, J. L. Weiland, N. Jarosik, G. Hinshaw, N. Odegard, K. M. Smith, R. S. Hill, B. Gold, M. Halpern *et al.*, Astrophys. J. Suppl. Ser. **208**, 20 (2013).
[3] J. Tauber (Planck Collaboration), Astron. Astrophys., doi:10.1051/0004-6361/201321529 (2013).
[4] V. Pettorino, Phys. Rev. D **88**, 063519 (2013).
[5] D. Hanson *et al.* (SPTpol Collaboration), Phys. Rev. Lett. **111**, 141301 (2013).
[6] P. Ade *et al.* (POLARBEAR Collaboration), Phys. Rev. Lett. **113**, 021301 (2014).
[7] P. Ade *et al.* (BICEP2 Collaboration), Phys. Rev. Lett. **112**, 241101 (2014).
[8] H. Liu, P. Mertsch, and S. Sarkar, Astrophys. J. **789**, L29 (2014).
[9] P. A. R. Ade, M. I. R. Alves, G. Aniano, C. Armitage-Caplan, M. Arnaud, F. Atrio-Barandela, J. Aumont, C. Baccigalupi, A. J. Banday *et al.* (Planck Collaboration), arXiv:1405.0874.
[10] L. Amendola, V. Pettorino, C. Quercellini, and A. Vollmer, Phys. Rev. D **85**, 103008 (2012).
[11] T. Giannantonio, Nucl. Phys. B, Proc. Suppl. **194**, 224 (2009).
[12] V. Acquaviva and C. Baccigalupi, Phys. Rev. D **74**, 103510 (2006).
[13] V. Acquaviva, C. Baccigalupi, and F. Perrotta, Phys. Rev. D **70**, 023515 (2004).
[14] A. Lewis and A. Challinor, Phys. Rep. **429**, 1 (2006).
[15] E. Macaulay, I. K. Wehus, and H. K. Eriksen, Phys. Rev. Lett. **111**, 161301 (2013).
[16] P. A. R. Ade, N. Aghanim, C. Armitage-Caplan, M. Arnaud, M. Ashdown, F. Atrio-Barandela, J. Aumont, C. Baccigalupi, A. J. Banday *et al.* (Planck Collaboration), arXiv:1303.5076.
[17] L. Amendola and S. Tsujikawa, *Dark Energy: Theory and Observations* (Cambridge University Press, Cambridge, England, 2010).
[18] T. Clifton, P. G. Ferreira, A. Padilla, and C. Skordis, Phys. Rep. **513**, 1 (2012).
[19] J. Yoo and Y. Watanabe, Int. J. Mod. Phys. D **21**, 1230002 (2012).
[20] G. W. Horndeski, Int. J. Theor. Phys. **10**, 363 (1974).
[21] C. Deffayet, X. Gao, D. Steer, and G. Zahariade, Phys. Rev. D **84**, 064039 (2011).
[22] S. Hassan and R. A. Rosen, J. High Energy Phys. 02 (2012) 126.
[23] E. Bellini and I. Sawicki, J. Cosmol. Astropart. Phys. 07 (2014) 050.
[24] L. Amendola, M. Kunz, M. Motta, I. D. Saltas, and I. Sawicki, Phys. Rev. D **87**, 023501 (2013).
[25] A. De Felice, T. Kobayashi, and S. Tsujikawa, Phys. Lett. B **706**, 123 (2011).
[26] F. Könnig and L. Amendola, arXiv:1402.1988.
[27] A. R. Solomon, Y. Akrami, and T. S. Koivisto, arXiv:1404.4061.
[28] A. De Felice and S. Tsujikawa, J. Cosmol. Astropart. Phys. 02 (2012) 007.

[29] I. D. Saltas, I. Sawicki, L. Amendola, and M. Kunz, arXiv:1406.7139.
[30] C. M. Caves, Ann. Phys. (N.Y.) **125**, 35 (1980).
[31] G. D. Moore and A. E. Nelson, J. High Energy Phys. 09 (2001) 023.
[32] R. Kimura and K. Yamamoto, J. Cosmol. Astropart. Phys. 7 (2012) 050.
[33] A. S. Goldhaber and M. M. Nieto, Rev. Mod. Phys. **82**, 939 (2010).
[34] Y.-F. Cai and Y. Wang, Phys. Lett. B **735**, 108 (2014).
[35] T. Matsumura, Y. Akiba, J. Borrill, Y. Chinone, M. Dobbs, H. Fuke, A. Ghribi, M. Hasegawa, K. Hattori, M. Hattori *et al.*, J. Low Temp. Phys. **176**, 733 (2014).
[36] C. Carbone, M. Baldi, V. Pettorino, and C. Baccigalupi, J. Cosmol. Astropart. Phys. 09 (2013) 004.
[37] C. Antolini, M. Martinelli, Y. Fantaye, and C. Baccigalupi, J. Cosmol. Astropart. Phys. 02 (2013) 024.
[38] T. Multamäki and Ø. Elgarøy, Astron. Astrophys. **423**, 811 (2004).
[39] Z. Hou, C. Reichardt, K. Story, B. Follin, R. Keisler *et al.*, Astrophys. J. **782**, 74 (2014).
[40] Z. Hou, R. Keisler, L. Knox, M. Millea, and C. Reichardt, Phys. Rev. D **87**, 083008 (2013).
[41] F. Simpson, C. Heymans, D. Parkinson, C. Blake, M. Kilbinger, J. Benjamin, T. Erben, H. Hildebrandt, H. Hoekstra, T. D. Kitching *et al.*, Mon. Not. R. Astron. Soc. **429**, 2249 (2013).
[42] A. Lewis and S. Bridle, Phys. Rev. D **66**, 103511 (2002).
[43] M. Hazumi, J. Borrill, Y. Chinone, M. A. Dobbs, H. Fuke, A. Ghribi, M. Hasegawa, K. Hattori, M. Hattori, W. L. Holzapfel *et al.*, in *Society of Photo-Optical Instrumentation Engineers (SPIE) Conference Series*, Vol. 8442 (SPIE-International Society for Optical Engineering, Bellingham, WA, 2012).
[44] J. Bock, A. Aljabri, A. Amblard, D. Baumann, M. Betoule, T. Chui, L. Colombo, A. Cooray, D. Crumb, P. Day *et al.*, arXiv:0906.1188.
[45] A. Kogut, D. J. Fixsen, D. T. Chuss, J. Dotson, E. Dwek, M. Halpern, G. F. Hinshaw, S. M. Meyer, S. H. Moseley, M. D. Seiffert *et al.*, J. Cosmol. Astropart. Phys. 07 (2011) 025.
[46] P. Andre, C. Baccigalupi, D. Barbosa, J. Bartlett, N. Bartolo, E. Battistelli, R. Battye, G. Bendo, J.-P. Bernard *et al.* (PRISM Collaboration), arXiv:1306.2259.
[47] C. Armitage-Caplan, M. Avillez, D. Barbosa, A. Banday, N. Bartolo, R. Battye, J. Bernard, P. de Bernardis, S. Basak *et al.* (COrE Collaboration), arXiv:1102.2181.
[48] G. Hinshaw, D. Larson, E. Komatsu, D. N. Spergel, C. L. Bennett, J. Dunkley, M. R. Nolta, M. Halpern, R. S. Hill, N. Odegard *et al.*, Astrophys. J. Suppl. Ser. **208**, 19 (2013).
[49] S. Das, T. Louis, M. R. Nolta, G. E. Addison, E. S. Battistelli, J. Bond, E. Calabrese, D. C. M. J. Devlin, S. Dicker, J. Dunkley *et al.*, J. Cosmol. Astropart. Phys. 04 (2014) 014.
[50] C. L. Reichardt, L. Shaw, O. Zahn, K. A. Aird, B. A. Benson, L. E. Bleem, J. E. Carlstrom, C. L. Chang, H. M. Cho, T. M. Crawford *et al.*, Astrophys. J. **755**, 70 (2012).
[51] S. Naess, M. Hasselfield, J. McMahon, M. D. Niemack, G. E. Addison, P. A. R. Ade, R. Allison, M. Amiri, A. Baker, N. Battaglia *et al.*, arXiv:1405.5524.
[52] L. Amendola and S. Tsujikawa, *Dark Energy: Theory and Observations* (Cambridge University Press, Cambridge, 2010).
[53] T. Kobayashi, M. Yamaguchi, and J. Yokoyama, Prog. Theor. Phys. **126**, 511 (2011).
[54] X. Gao and D. A. Steer, J. Cosmol. Astropart. Phys. 12 (2011) 019.
[55] A. De Felice and S. Tsujikawa, Phys. Rev. D **84**, 083504 (2011).
[56] S. Tsujikawa, J. Ohashi, S. Kuroyanagi, and A. De Felice, Phys. Rev. D **88**, 023529 (2013).
[57] F. Koennig, Y. Akrami, L. Amendola, M. Motta, and A. R. Solomon, arXiv:1407.4331.
[58] M. Raveri, A. Silvestri, and S.-Y. Zhou, arXiv:1405.7974.